Mouse Apg16L, a novel WD-repeat protein, targets to the autophagic isolation membrane with the Apg12-Apg5 conjugate

Noboru Mizushima[1,2,*], Akiko Kuma[2,3], Yoshinori Kobayashi[2,3], Akitsugu Yamamoto[4], Masami Matsubae[5], Toshifumi Takao[5], Tohru Natsume[6], Yoshinori Ohsumi[2,3,*] and Tamotsu Yoshimori[2,3,7]

[1]PRESTO, Japan Science and Technology Corporation, Kawaguchi 332-0012, Japan
[2]Department of Cell Biology, National Institute for Basic Biology, 38 Nishigonaka, Myodaiji, Okazaki 444-8585, Japan
[3]Department of Molecular Biomechanics, School of Life Science, The Graduate University for Advanced Studies, Okazaki 444-8585, Japan
[4]Department of Physiology, Kansai Medical University, Moriguchi 570-8506, Japan
[5]Institute for Protein Research, Osaka University, Yamadaoka 3-2, Suita, Osaka 565-0871, Japan
[6]National Institute of Advanced Industrial Science and Technology, Tokyo 135-0064, Japan
[7]Department of Cell Genetics, National Institute of Genetics, Mishima 411-8540, Japan
*Authors for correspondence (e-mail: nmizu@nibb.ac.jp; yohsumi@nibb.ac.jp)

Accepted 21 January 2003
Journal of Cell Science 116, 1679-1688 © 2003 The Company of Biologists Ltd
doi:10.1242/jcs.00381

Summary

Macroautophagy is the major intracellular degradation system delivering cytoplasmic components to the lysosome/vacuole. We have shown that, in yeast and mammalian cells, the Apg12-Apg5 protein conjugate, which is formed by a ubiquitin-like system, is essential for autophagosome formation. In yeast, the Apg12-Apg5 conjugate interacts with a small coiled-coil protein, Apg16, to form a ~350 kDa multimeric complex. We demonstrate that the mouse Apg12-Apg5 conjugate forms a ~800 kDa protein complex containing a novel WD-repeat protein. Because the N-terminal region of this novel protein shows homology with yeast Apg16, we have designated it mouse Apg16-like protein (Apg16L). Apg16L, however, has a large C-terminal domain containing seven WD repeats that is absent from yeast Apg16. Apg16L interacts with both Apg5 and additional Apg16L monomers; neither interaction, however, depends on the WD-repeat domain. In conjunction with Apg12-Apg5, Apg16L associates with the autophagic isolation membrane for the duration of autophagosome formation. Because these features are similar to yeast Apg16, we concluded Apg16L is the functional counterpart of the yeast Apg16. We also found that membrane targeting of Apg16L requires Apg5 but not Apg12. Because WD-repeat proteins provide a platform for protein-protein interactions, the ~800 kDa complex is expected to function in autophagosome formation, further interacting with other proteins in mammalian cells.

Key words: Autophagy, Apg12, Apg5, WD repeat

Introduction

Macroautophagy (referred to as autophagy hereafter) mediates the bulk degradation of cytoplasmic components in the lysosome/vacuole. This system is implicated in protein turnover, the starvation response, cellular differentiation and cell death (Seglen and Bohley, 1992; Dunn, 1994; Blommaart et al., 1997; Klionsky and Emr, 2000). Autophagy accounts for the degradation of most long-lived proteins and some organelles; cytoplasmic constituents, including organelles, are sequestered into double-membraned autophagosomes, which subsequently fuse with lysosomes. Yeast genetic screens have identified at least 16 genes (*APG* and *AUT* genes) required for autophagosome formation (Tsukada and Ohsumi, 1993; Thumm et al., 1994). Among these, we identified two novel ubiquitin-like conjugation systems (Ohsumi, 2001). In the Apg12 conjugation system, the C-terminal glycine of Apg12 is covalently attached to a lysine at the center of Apg5 (Mizushima et al., 1998a). Apg7 and Apg10 serve to catalyze the conjugating reaction (Tanida et al., 1999; Kim et al., 1999; Shintani et al., 1999). The Aut7/Apg8 system, in which Aut7 is conjugated to phosphatidylethanolamine, is catalyzed by Apg7 and Aut1/Apg3 (Kirisako et al., 2000; Ichimura et al., 2000). These two conjugation systems are highly conserved in mammals (Mizushima et al., 1998b; Mizushima et al., 2002a; Mizushima et al., 2002b; Kabeya et al., 2000; Tanida et al., 2001; Tanida et al., 2002). Indeed, we demonstrated that mouse Apg5 is indispensable for mammalian autophagy (Mizushima et al., 2001). Recent studies in yeast and mammalian cells suggested that the Apg12-Apg5 conjugate and Aut7 (LC3 in mammalian cells) localize to autophagosome precursors and play major roles in the development of autophagic isolation membranes into autophagosomes (Suzuki et al., 2001; Mizushima et al., 2001). Apg12-Apg5 dissociates from the autophagosomal membrane upon completion of autophagosome formation, while Aut7/LC3 remains on the autophagosomal membrane. Cells deficient in the Apg12 conjugation system are defective in Aut7/LC3 modification and membrane targeting, suggesting that the functions of these two ubiquitin-like systems are closely related (Suzuki et al., 2001; Mizushima et al., 2001). In addition, these two systems are implicated in the microautophagy of peroxisomes (Yuan et al., 1999; Mukaiyama et al., 2002).

Although Apg12-Apg5 functions to elongate the isolation membrane, most Apg12-Apg5 exists freely in the cytosol (Mizushima et al., 2001; Kuma et al., 2002). In yeast, the Apg12-Apg5 conjugate further interacts with a small coiled-coil protein, Apg16 (Mizushima et al., 1999). Apg16 forms a homo-oligomer through its coiled-coil region. As each Apg16 molecule interacts with Apg5, Apg16 homo-oligomers cross-link multiple Apg12-Apg5 conjugates. As a result, Apg12-Apg5 and Apg16 form a ~350 kDa protein complex thought to contain four sets of Apg12-Apg5 and Apg16 (Kuma et al., 2002). We have demonstrated that the formation of this ~350 kDa complex is essential for autophagy. In addition, we determined that Apg16 is localized to the preautophagosomal structure and is required for membrane targeting of Apg5 (Suzuki et al., 2001). As yet, no molecules structurally related to Apg16 have been found in other species through database analysis. Because the structure and function of the Apg12-Apg5 conjugate is well conserved in mammals, we postulated the existence of a functional Apg16 counterpart. In this study, we demonstrate that, in mammalian cells, Apg12-Apg5 forms an 800 kDa protein complex with a novel WD-repeat protein. Because biochemical and morphological analyses suggested that it is the mammalian counterpart of yeast Apg16, we named it Apg16L (Apg16-like protein). The C-terminal WD-repeat domain, however, is found only in Apg16L. Because the WD-repeat domain mediates protein-protein interactions, Apg16L might function as a scaffold for a protein complex functioning in autophagosome formation.

Materials and Methods

Cell culture and transfections

Wild-type (a gift from Andras Nagy) and genetically manipulated R1 embryonic stem (ES) cells were cultured either on mitomycin-C-treated embryonic fibroblasts or on gelatinized dishes in a complete ES medium as described (Mizushima et al., 2001). The generation of *APG5*$^{-/-}$ ES cells and various stable transformants (GFP24 and GKR-1) have previously been described (Mizushima et al., 2001). HeLa cells were cultured in Dulbecco's modified Eagle's medium (Sigma) supplemented with 10% fetal bovine serum (Gibco). To starve cells of amino acids, cells were cultured in Hanks' solution containing 10 mM Hepes, pH 7.5 (without amino acids and fetal bovine serum). Transient transfections were performed using LipofectAMINE 2000 reagent (Life Technologies). Transfected cells were processed for immunoblotting or immunoprecipitation 18 hours after transfection. To obtain stable transformants, 8×10^6 ES cells were electroporated with 20 μg of linearized plasmid, with the addition of 2 μg of pPGKpurobpA when required. Cells were selected in the presence of either 1 mg ml^{-1} G418 or 5 μg ml^{-1} puromycin.

Immunoprecipitation

Cells grown on 35 mm dishes were labeled with 0.4 mCi of [^{35}S]methionine/cysteine (NEN Life Science Products) for 2 hours when indicated. After cells were lysed in lysis buffer (2% NP-40 in PBS supplemented with protease inhibitors) for 20 minutes, the nuclear and cellular debris was cleared by centrifugation. Immunoprecipitation was performed using rabbit polyclonal anti-green-fluorescent-protein (GFP; MBL), mouse monoclonal anti-FLAG (M2) (Sigma) or anti-hemagglutinin (HA) antibody (16B12) (Babco) and protein-A/Sepharose or protein-G/Sepharose (Amersham Biosciences). Immunoprecipitates were washed six times in lysis buffer and eluted in SDS sample buffer. Proteins were separated by SDS-PAGE and analyzed by either a bioimage analyser BAS2000 (Fuji Film) or immunoblotting as described (Mizushima et al., 1998b).

Protein purification and mass spectrometry

Total cell lysates were prepared from 10-20 15 cm dishes of ES cells. The protein complex containing GFP-Apg5 was purified by passing the lysates over an anti-GFP-antibody-coupled protein-A/Sepharose bead column. After extensive washing, bound proteins were eluted in 0.1 M glycine-HCl (pH 2.5), separated by SDS-PAGE and visualized with Coomassie Brilliant Blue or silver staining. Following excision from the gels, proteins of 63 kDa and 71 kDa were digested in situ with lysyl-endopeptidase or trypsin. The resultant peptides were subjected to matrix-assisted laser desorption ionization (MALDI) mass spectrometry (MS). Proteins were identified by database searching based on their peptide masses. For further unambiguous protein identification, the same bands were digested with lysyl-endopeptidase and then analysed by the direct nano-liquid-chromatography tandem MS system (Natsume et al., 2002) in conjunction with searches of the NCBInr database using Mascot software.

Plasmids

The cDNA corresponding to the open reading frame of mouse Apg16Lα was obtained by polymerase chain reaction of IMAGE consortium clone 1480862 (GenBank accession number AI037166). This fragment was then cloned into the *Sal*I site of pCI-neo (Promega), the *Xba*I site of p3XFLAG-CMV-10 (Sigma) and the *Sal*I sites of pEGFP-C1, pECFP-C1 and pEYFP-C1 (Clontech) to generate pCI-Apg16L, pFLAG-Apg16L, pEGFP-Apg16L, pECFP-Apg16L and pEYFP-Apg16L, respectively. The mouse Apg5 and rat LC3 cDNAs were also subcloned into pECFP-C1 (pECFP-Apg5) and pEYFP-C1 (pEYFP-LC3). To attain better expression in ES cells, the Apg16L, FLAG-Apg16L, EGFP-Apg16L, ECFP-Apg16L and EYFP-Apg16L fragments were also subcloned into pCE-FL (a gift from S. Sugano), a vector containing a cytomegalovirus enhancer and elongation factor promotor. pApg5-HA and pEGFP-Apg5 constructs have been described previously (Mizushima et al., 1998b; Mizushima et al., 2001). For yeast two-hybrid analysis, various regions of the Apg16Lα cDNA corresponding to amino acids 1-588 (full length), 1-276, 1-79, 72-276 and 219-588 were cloned into the *Sal*I sites of pGBD-C1 and pGAD-C1. The mouse Apg5 cDNA was also cloned into the *Sma*I sites of pGBD-C1 and pGAD-C1. For expression of glutathione-*S*-transferase (GST)-tagged Apg16Lα (219-588) in *Escherichia coli*, a cDNA encoding amino acids 219-588 of Apg16Lα was first cloned into the *Sal*I site of pENT1A from the GATEWAY cloning system (Invitrogen). A GST-Apg16L (219-588) expression plasmid (pDEST15-Apg16LC) was then generated according to the manufacturer's instructions.

Generation of antibody against mouse Apg16L

To generate an antibody against mouse Apg16L (p63C-2), pDEST15-Apg16LC was transformed into BL21-SI competent cells (Invitrogen). Expression of C-terminal half of Apg16L fused to GST was induced for 2 hours with 0.3 M NaCl. The recombinant protein, contained in inclusion bodies, was separated by SDS-PAGE and isolated as previously described (Kuma et al., 2002). The eluted protein was then used to immunize rabbits.

Reverse-transcription PCR

Total RNA isolated from mouse liver, brain, kidney, ES cells and HeLa cells was subjected to reverse transcription using a ProSTAR™ First-Strand RT-PCR kit (Stratagene). A part of the Apg16L cDNA corresponding to exons 6-10 was amplified with primers p63-4Bam

(5′-ACGTGGATCCAGGAGGCGTCAAGCACGGCTG-3′) and p63-22Sal (5′-GAACGTGTCGACCTGGGGGACTGGGATGGAAGAG-AC-3′).

Yeast two-hybrid assay

The two-hybrid analysis was performed as described (James et al., 1996). The strain PJ69-4A was co-transformed with one of each of the pGBD and pGAD plasmids. Transformants were selected on SC –Trp –Leu plates and tested for growth on SC –His –Trp –Leu plates containing 3 mM 3-amino-triazole (3-AT).

Differential centrifugation and gel filtration

The liver and brain of a C57BL/6N Crj mouse were homogenized in nine volumes of ice-cold PBS supplemented with protease inhibitors. ES cells were lysed in lysis buffer [50 mM Tris-HCl (pH 7.5), 150 mM NaCl and protease inhibitors] by passing the solution through a polycarbonate filter with 5-μm pores (Whatman). After a preclearing step at 100 ***g*** for 5 minutes, lysates were subjected to low-speed centrifugation at 13,000 ***g*** for 20 minutes to generate a pellet (P13) fraction. The resulting supernatant was further centrifuged at 100,000 ***g*** for 1 hour to generate pellet (P100) and supernatant (S100) fractions. The S100 fraction (~0.3 mg protein in 200 μl) was then applied to a Superose 6 column (Amersham Biosciences) and eluted at a flow rate of 0.4 ml min^{-1} with 50 mM Tris, pH 7.5, 150 mM NaCl, 1 mM DTT. 0.6 ml fractions were then examined by immunoblotting. The column was calibrated with gel filtration protein standards (Amersham Biosciences) containing thyroglobulin (669 kDa), ferritin (440 kDa), catalase (232 kDa) and albumin (67 kDa).

Fluorescence microscopy

ES cells expressing protein fused to GFP, yellow fluorescent protein (YFP) or cyan fluorescent protein (CFP) were directly observed with a DeltaVision microscope system (Applied Precision Incorporation). For examination by immunofluorescence microscopy, ES cells grown on gelatinized coverslips were fixed and stained with an anti-mouse Apg16L antibody (200× dilution) and a Cy5-conjugated goat anti-rabbit IgG antibody (Amersham Biosciences). Samples were examined under a fluorescence laser scanning confocal microscope, LSM510 (Carl Zeiss) as previously described (Yoshimori et al., 2000).

Electron microscopy

ES cells, grown on gelatinized plastic coverslips, were fixed for 2 hours with 4% paraformaldehyde in 0.1 M cacodylate buffer, pH 7.4, and then subjected to the pre-embedding silver-enhancement immunogold method for immunoelectron microscopy using an antibody against GFP (Mizushima et al., 2001).

Results

Identification of Apg16L

Although the Apg12-Apg5 conjugate is essential for elongation of the isolation membrane, most Apg12-Apg5 is present in the cytosol of both yeast and mammalian cells (Kuma et al., 2002; Mizushima et al., 2001). In yeast, Apg16 forms a ~350 kDa multimeric complex with Apg12-Apg5 (Kuma et al., 2002). To determine the involvement of mammalian Apg12-Apg5 in such a large complex, S100 fractions of various mouse tissues were subjected to gel filtration analysis using a Superose 6 column. The Apg12-Apg5 conjugate was eluted in a single fraction peak corresponding to ~800 kDa, much larger than the yeast Apg12-Apg5·Apg16 complex (see below and Fig. 5). Therefore, mammalian Apg12-Apg5 likely forms a protein complex with additional protein(s).

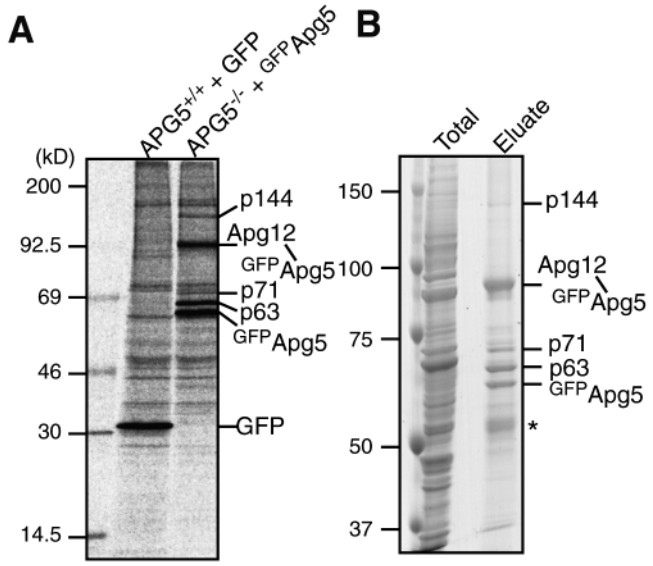

Fig. 1. Identification of proteins interacting with Apg5 in mouse ES cells. (A) Wild-type ES cells stably expressing GFP alone and Apg5-deficient ES cells stably expressing GFP-fused Apg5 (GFP24) were labeled with [^{35}S]methionine/cysteine for 2 hours. Following immunoprecipitation with anti-GFP antibody from cell lysates, the immunoprecipitates were analyzed by SDS-PAGE and a bioimage analyzer. (B) Purification of Apg5-interacting proteins. Total cell lysates were prepared from GFP24 cells and subjected to affinity purification using an anti-GFP antibody-coupled protein-A/Sepharose bead column. Following elution, bound proteins were separated by SDS-PAGE and stained with Coomassie Brilliant Blue. The positions of unconjugated GFP-Apg5, Apg12/GFP-Apg5, and three unknown proteins of 63 kDa, 71 kDa and 144 kDa are indicated. Asterisk indicates the position of immunoglobulin heavy chain partially dissociated from the column.

As the ~800 kDa complex is also detected in *APG5*$^{-/-}$ mouse ES cells stably expressing GFP-fused Apg5 (clone GFP24) (Mizushima et al., 2001) (data not shown), we identified additional subunits of this complex by co-immunoprecipitation using an antibody against GFP. Anti-GFP immunoprecipitates from total cell lysate of ^{35}S-labeled GFP24 cells contained several specific proteins of 63 kDa, 71 kDa and 144 kDa, in addition to GFP-Apg5 and Apg12/GFP-Apg5 (Fig. 1A). These proteins were not present in precipitates from wild-type ES cells expressing GFP alone.

To identify these proteins, cell lysates derived from GFP24 ES cells were passed over an anti-GFP antibody-coupled protein-A/Sepharose column. Bound proteins were eluted and separated by SDS-PAGE (Fig. 1B). Coomassie-stained gel bands corresponding to p63 and p71were digested in situ with lysyl-endopeptidase or trypsin. MS protein identification revealed that both p63 and p71 represent a novel protein (isoforms, see below), predicted by several expressed sequence tags (ESTs; AI037166, BI687378, BB620083, AA982950, BE3714456, BB660407, BB839395, BB853783 etc.) (Fig. 2A). This protein contains a coiled-coil region at the N-terminal region (amino acids 91-190) and seven WD repeats,

which are implicated in protein-protein interactions (Smith et al., 1999), in the C-terminus (outlined in black in Fig. 2A). Although this protein is much larger than yeast Apg16, the N-terminal region (amino acids 106-208) demonstrated a weak but significant homology with yeast Apg16 (amino acids 28-145) (22% identity and 43% similarity) (Fig. 2B). Therefore, we tentatively named it Apg16L (Apg16-like protein). Putative Apg16L homologues are present in various eukaryotes, but are not present in *Saccharomyces cerevisiae* (Fig. 2C).

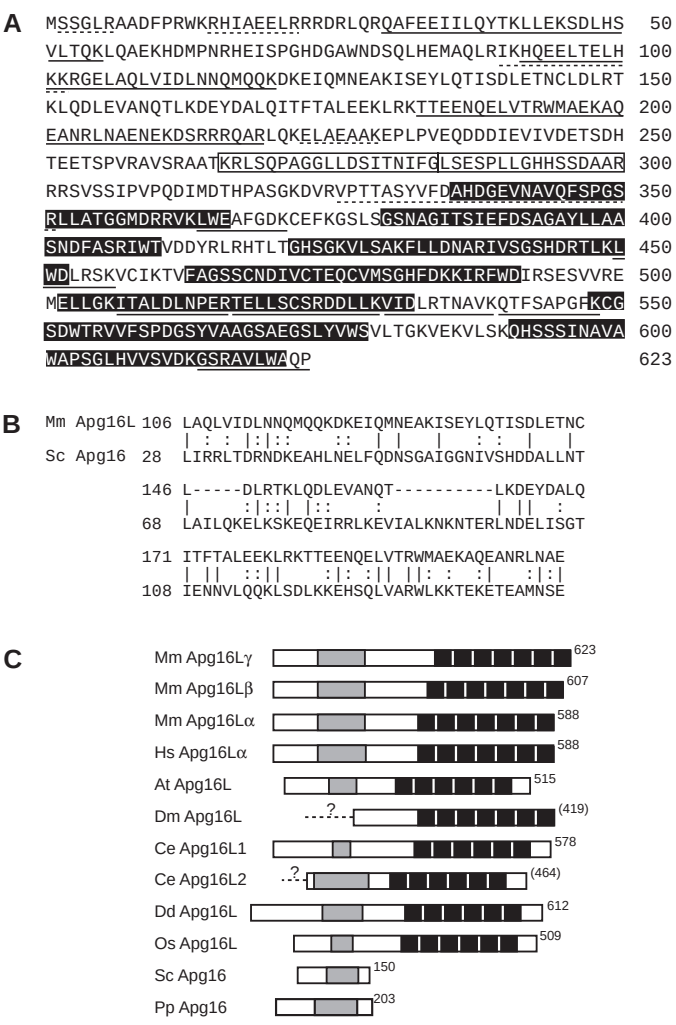

Fig. 2. Structure of Apg16L. (A) Amino acid sequence of Apg16L. Underlined and dotted-underlined residues correspond to peptide sequences obtained by MS analysis of p63 and p71, respectively. Boxes indicate the peptides encoded by exons 8 and 9, which are deleted in spliced isoforms. Sequences outlined in black are WD repeats. (B) Amino acid sequence of mouse Apg16L was aligned with that of *S. cerevisiae* Apg16 using the BLAST2 program (http://www.ncbi.nlm.nih.gov/blast/bl2seq/bl2.html). Identical amino acids are shown with a line between them (|), while similar amino acids are indicated with dots (:). (C) Structural comparison of putative Apg16L homologues. The coiled-coil regions are indicated as gray boxes [analyzed by Multicoil program (Wolf et al., 1997), http://multicoil.lcs.mit.edu/cgi-bin/multicoil] and the WD repeats are shown as black boxes (analyzed by PSA Sequence analysis, http://bmerc-www.bu.edu/psa/request.htm). At, *Arabidopsis thaliana* (AB024031); Ce, *Caenorhabditis elegance* (U53340, U23449); Dd, *Dictyostelium discoideum* (AF019236); Dm, *Drosophila melanogaster* (AY058742); Hs, *Homo sapiens* (AK027854, AK024453); Mm, *Mus musculus*; Os, *Oryza sativa* (AC087852); Pp, *Pichia pastoris* (Mukaiyama et al., 2002) (Y. Sakai, personal communication); Sc, *Saccharomyces cerevisiae*. The amino acid sequences of Dm Apg16L and Ce Apg16L2, hypothesized from the genomic sequences, might be incomplete, lacking N-terminal sequences.

Spliced isoforms of Apg16L

We generated polyclonal antibodies against the C-terminal region of mouse Apg16L. Immunoblot analysis of mouse tissue demonstrated that Apg16L was expressed ubiquitously (Fig. 3B, data not shown for heart, spleen, thymus, testis). The size of Apg16L, however, differed among the tissues and cell lines tested. The liver, kidney (Fig. 3B), spleen, thymus and testes (data not shown) contained a major form of 63 kDa with a minor form of 71 kDa. This expression pattern, consistent with the results of immunoprecipitation and affinity purification using anti-GFP antibody (Fig. 1), was also observed in ES cells (Fig. 3B). By contrast, a larger 75 kDa form was the most abundant species in brain, skeletal muscle (Fig. 3B) and heart (data not shown). Both the 63 kDa and 71 kDa proteins were the major forms in HeLa cells. The genomic DNA sequence and the cDNA sequences of the EST database suggested that the *APG16L* gene encodes multiple isoforms. We confirmed by sequence analysis that at least three isoforms of Apg16L were generated by alternative splicing events (Fig. 3A). The major cDNA present in the liver, designated Apg16Lα, lacks all of exons 8 (57 bp) and 9 (48 bp). The minor cDNA present in the liver, designated Apg16Lβ, lacks exon 9. The major cDNA present in the brain, designated Apg16Lγ, contains the complete sequences of both exons 8 and 9. The peptides encoded by exons 8 and 9, deleted in Apg16Lα and Apg16Lβ, are located between the coiled-coil region and WD repeat. Transient transfection of the Apg16Lα cDNA into HeLa cells increased the levels of p63 (Fig. 3B, lane 7). Therefore, the p63 and p71 proteins affinity purified from ES cell lysates represented Apg16Lα and Apg16Lβ, respectively. The reverse-transcription-PCR pattern amplifying exons 8 and 9 is shown in Fig. 3C.

Apg16L interacts with Apg5 and Apg16L itself

The isolation of mouse Apg16L from the Apg5 complex suggests that Apg16L has a function similar to yeast Apg16. We thus examined the interaction of Apg16L with Apg5. HeLa cells were transiently transfected with FLAG-tagged mouse Apg16Lα and/or HA-tagged Apg5. Immunoprecipitation analysis using anti-FLAG or anti-HA antibody revealed that Apg16L and Apg5 were specifically co-precipitated (Fig. 4A). Both Apg12-conjugated and unconjugated Apg5 were immunoprecipitated with the anti-FLAG antibody, suggesting that Apg16L interacts directly with Apg5 but not with Apg12. We determined the specific Apg5-binding domain of Apg16L using a yeast two-hybrid assay. The extreme N-terminal region of Apg16L (amino acids 1-79), upstream of the coiled-coil region, was sufficient to interact with Apg5 (Fig. 4C). This result is consistent with the interaction of yeast Apg16 with yeast Apg5 through the corresponding region (Mizushima et al., 1999). We also observed that the N-terminal region of Apg16L (amino acids 1-276) homodimerizes (Fig. 4C),

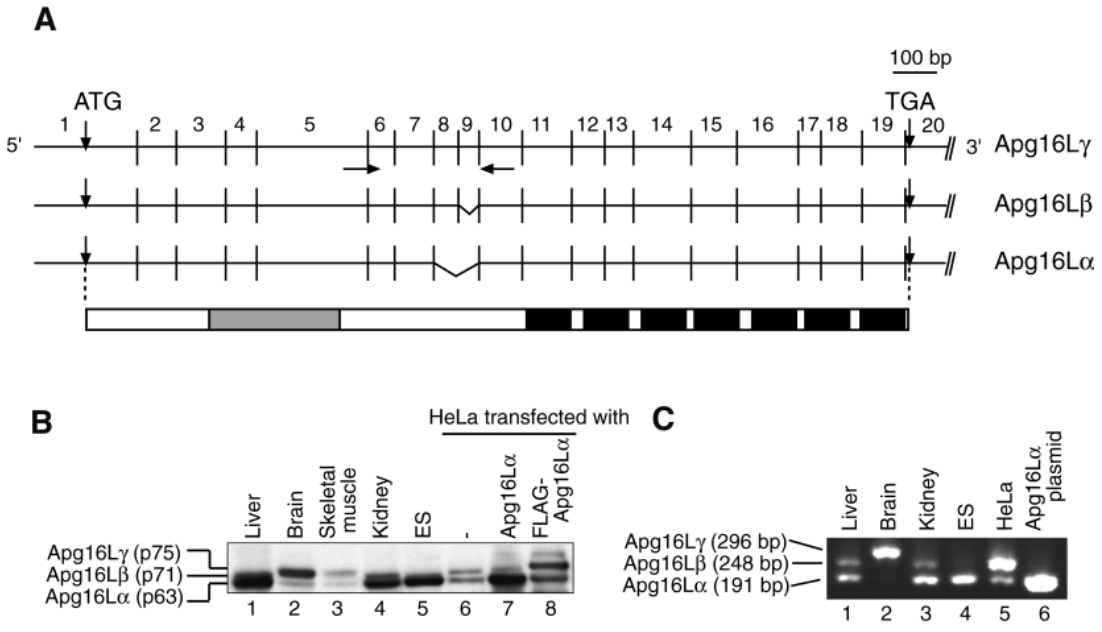

Fig. 3. Spliced isoforms of Apg16L. (A) Alternative splicing of Apg16L mRNA. The 20 exons are indicated by numbers above the line representing Apg16Lγ. Alternatively spliced exons in Apg16Lα and Apg16Lβ are indicated as broken lines. The positions of the primers (within exons 6 and 10) used in C are indicated by arrows. Corresponding domain structures are shown as in Fig. 2C. (B) Expression of Apg16L in tissues and cell lines. Tissue homogenates were prepared from mouse liver (lane 1), brain (lane 2), the gastrocnemius muscle (lane 3) and kidney (lane 4). Total cell lysates were also prepared from ES cells (lane 5) and HeLa cells transiently transfected with either vector alone (lane 6), Apg16Lα (lane 7) or FLAG-tagged Apg16Lα (lane 8). The mobility of the three isoforms is indicated. (C) Reverse-transcription-PCR analysis of Apg16L mRNA. Total RNA was isolated from mouse liver (lane 1), brain (lane 2), kidney (lane 3), ES cells (lane 4) and HeLa cells (lane 5), and reverse-transcribed into cDNA. A fragment of the Apg16L cDNA corresponding to exons 6-10 was amplified using the primers indicated in A. The cDNA sequences of mouse Apg16Lα, Apg16Lβ and Apg16Lγ have been deposited in the DDBJ/EMBL/GenBank databases under accession numbers AB087879, AB087880 and AB087881, respectively.

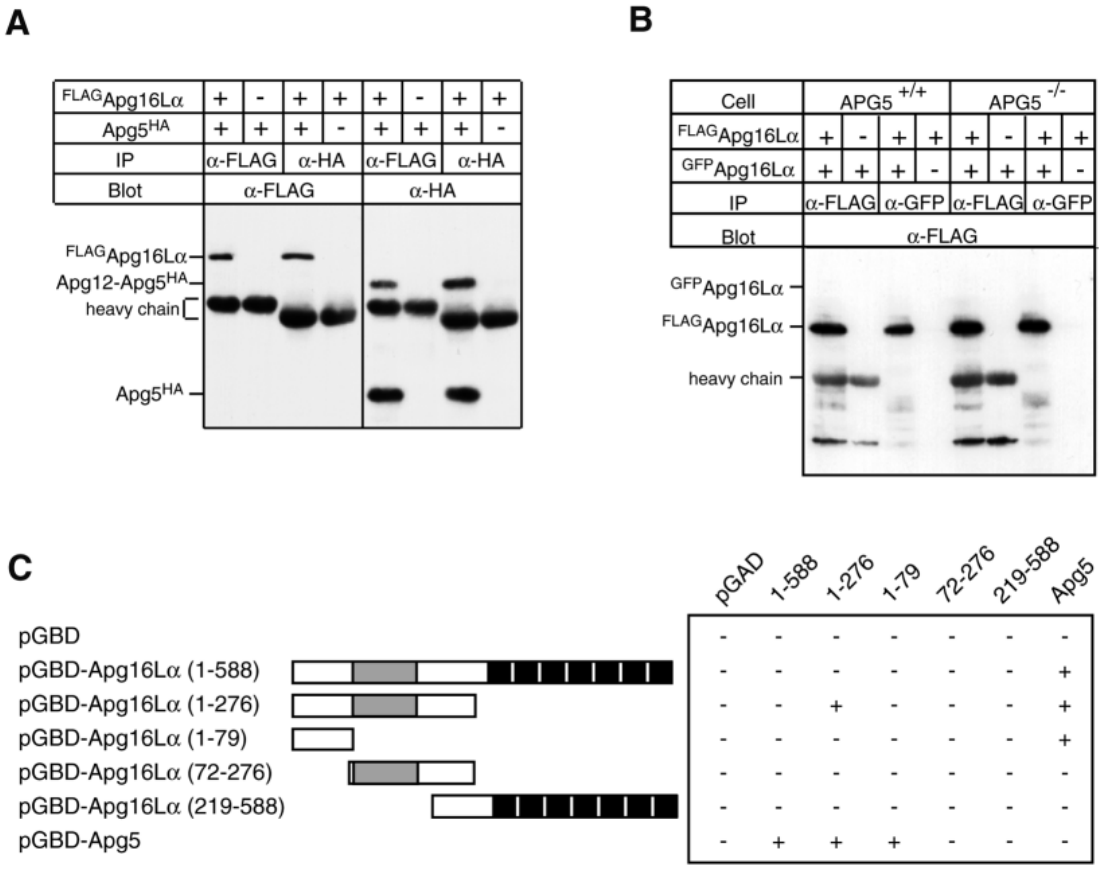

Fig. 4. Apg16L interacts with Apg5 and additional Apg16L monomers. (A) Apg16L interacts with Apg5. FLAG-tagged Apg16L and HA-tagged Apg5 were immunoprecipitated from HeLa cells transiently transfected with the indicated plasmids. The interaction of these co-transfected molecules was examined by western-blot analysis using anti-FLAG and anti-HA antibodies. (B) Apg16L forms a homo-oligomer. Wild-type ES cells and Apg5-deficient ES cells were transiently transfected with FLAG-tagged Apg16L and/or GFP-tagged Apg16L. Immunoprecipitates of GFP-Apg16L were examined for the co-immunoprecipitation of FLAG-Apg16L by western-blot analysis using anti-FLAG antibody. (C) Two-hybrid interactions of Apg16L-Apg5 and Apg16L-Apg16L. Interactions between Apg16L, Apg16L deletion constructs and Apg5 within transfected yeast cells were assessed for growth on SC –His –Trp –Leu plates containing 3 mM 3-amino-triazole.

although we could not determined the region required in greater detail. As yeast Apg16 forms homo-oligomers through its coiled-coil domain, we speculate that the coiled-coil domain of mouse Apg16L also self-associates. These data also demonstrated that the WD domain is not required for either Apg5 interaction or homo-oligomerization.

Although we could not detect full-length Apg16L homo-dimerization by two-hybrid analysis, this self-association was demonstrated by co-immunoprecipitation experiments in wild-type ES cells transiently expressing both GFP- and FLAG-tagged Apg16L. When GFP-tagged Apg16L was precipitated with an anti-GFP antibody, FLAG-tagged Apg16L was co-precipitated (Fig. 4B) and vice versa (data not shown). Apg16L self-interaction does not require Apg5, because similar results were obtained when using *APG5*$^{-/-}$ ES cells (Fig. 4B). Thus, Apg16L probably forms a homo-oligomer.

Apg12-Apg5 and Apg16L form a ~800 kDa protein complex

In yeast, Apg12-Apg5 forms a stable ~350 kDa protein complex with Apg16 in the cytosol (Kuma et al., 2002). We therefore examined the composition of the mammalian complex by probing for mammalian Apg12-Apg5 and Apg16L. As previously reported, in wild-type ES cells, almost all Apg5 was conjugated to Apg12, mainly recovered in the cytosolic fraction by differential centrifugation analysis (Mizushima et al., 2001). Apg16L was also primarily recovered in 100,000 ***g*** supernatants of both *APG5*$^{+/+}$ and *APG5*$^{-/-}$ ES-cell homogenates, suggesting that most Apg16L is present in the cytosol (Fig. 5A). Mouse tissues (liver, brain, kidney and testes) demonstrated similar results (data not shown). Although the presence of physiological salt concentrations in the lysis buffer is important in differential centrifugation experiments using yeast cell lysates (Kuma et al., 2002), the centrifugation results for mammalian cells were not affected by salt concentration (data not shown).

To determine the complex molecular mass, the 100,000 ***g*** fraction was then subjected to gel filtration analysis using a Superose 6 column; subsequent immunoblotting of eluate fractions with anti-Apg5 and anti-Apg16L antibodies determined the location of the complex. The Apg12-Apg5 conjugate from multiple tissues and cell lines eluted primarily in fractions corresponding to ~800 kDa, with an occasional minor peak observed at ~400 kDa (Fig. 5B). This result conflicted with the data obtained using yeast cells, in which Apg12-Apg5 and Apg16 form a ~350 kDa complex (Kuma et al., 2002). It is unlikely that components other than Apg12, Apg5 and Apg16L are contained in the mammalian ~800 kDa complex, because other stoichiometric subunits were not detected (Fig. 1). The amount of p144 precipitated with Apg5 was small enough that it would not contribute to the molecular mass of the complex. Considering the molecular mass of mouse Apg12 (15 kDa), Apg5 (32 kDa) and Apg16Lα (66 kDa), the ~800 kDa complex probably includes eight sets of Apg12-Apg5·Apg16L, whereas the ~400 kDa minor complex contains four sets.

The elution pattern of all three isoforms of mouse Apg16L was similar to that of Apg12-Apg5 (Fig. 5B): Apg16Lα and Apg16Lβ (liver and ES), and Apg16Lγ (brain). Co-elution of Apg12-Apg5 and Apg16L indicated that most of the Apg12-Apg5 conjugate and Apg16L are contained within the ~800 kDa protein complex. All three Apg16L isoforms can be recruited into the complex. Monomeric Apg12-Apg5 conjugate and Apg16L were not detected. Formation of the ~800 kDa complex was not affected by nutrient conditions (data not shown).

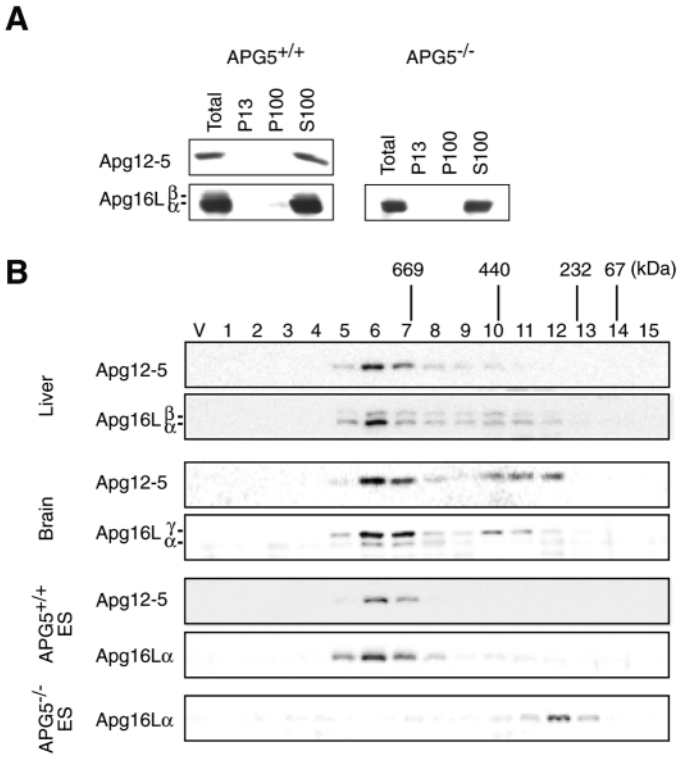

Fig. 5. Apg16L forms a ~800 kDa protein complex with Apg12-Apg5. (A) Apg16L is present primarily in the cytosol. ES cell homogenate (Total) was fractionated into an initial pellet (P13) and a subsequent pellet (P100) and supernatant (S100) fractions by differential centrifugation. These fractions were analysed by immunoblotting using antibodies against Apg5 and Apg16L. (B) Apg12-Apg5 and Apg16L form a ~800 kDa complex. S100 fractions of tissue homogenates of liver and brain, and cell lysates of wild-type and *APG5*$^{-/-}$ ES cells were separated by size exclusion chromatography on a Superose 6 column. Each fraction was subjected to immunoblotting using anti-Apg5 and anti-Apg16L antibodies. Positions of the molecular mass standards (in kDa) are shown. V, void fraction.

In *APG5*$^{-/-}$ ES cells, this ~800 kDa complex was not formed. Apg16L was recovered as a single peak in fractions corresponding to ~250 kDa, a size larger than the molecular mass of Apg16Lα monomer (Fig. 5B). We assume that the ~250 kDa complex in the *APG5*$^{-/-}$ ES cells represents a tetrameric Apg16L oligomer.

Apg16L localizes to autophagic isolation membrane

A small proportion of the cytosolic Apg12-Apg5 conjugate localizes to autophagic isolation membranes, playing an essential role in the elongation of the membrane. Thus, we examined the possible co-localization of Apg16L to the isolation membrane with Apg12-Apg5. We generated ES cells stably co-expressing combinations of fluorescently tagged

Apg5, Apg16L and LC3. LC3, a mammalian homologue of Aut7, serves as a molecular marker of autophagosomes (Kabeya et al., 2000). Upon the induction of autophagy by the withdrawal of serum and amino acids, YFP-LC3 associated with both isolation membranes and completely formed autophagosomal membranes. As autophagosome size in ES cells is larger than in other cell lines, LC3 labeling was often identified as a ring-shaped structure even when using conventional fluorescent microscopy (Fig. 6A, right). Apg5, however, was present only on the isolation membranes enclosing the cytoplasm, not on ring-shaped autophagosome structures (Fig. 6A, middle) (Mizushima et al., 2001). The subcellular localization of Apg16L was similar to Apg5; CFP-Apg5-positive isolation membranes clearly co-labeled with YFP-Apg16L (Fig. 6B). Although the Apg16L-labeled structure was positive for LC3, Apg16L never co-localized with the LC3-positive ring-shaped structures (Fig. 6C).

Apg5 is localized not only to cup-shaped isolation membranes but also to small crescent-shaped vesicles (Mizushima et al., 2001). Immunoelectron microscopy revealed that Apg16L associates extensively with small vesicles, considered to be isolation membranes in the early stages of formation (Fig. 7A,B). Although Apg16L associated with the membrane throughout isolation membrane development, its localization gradually became

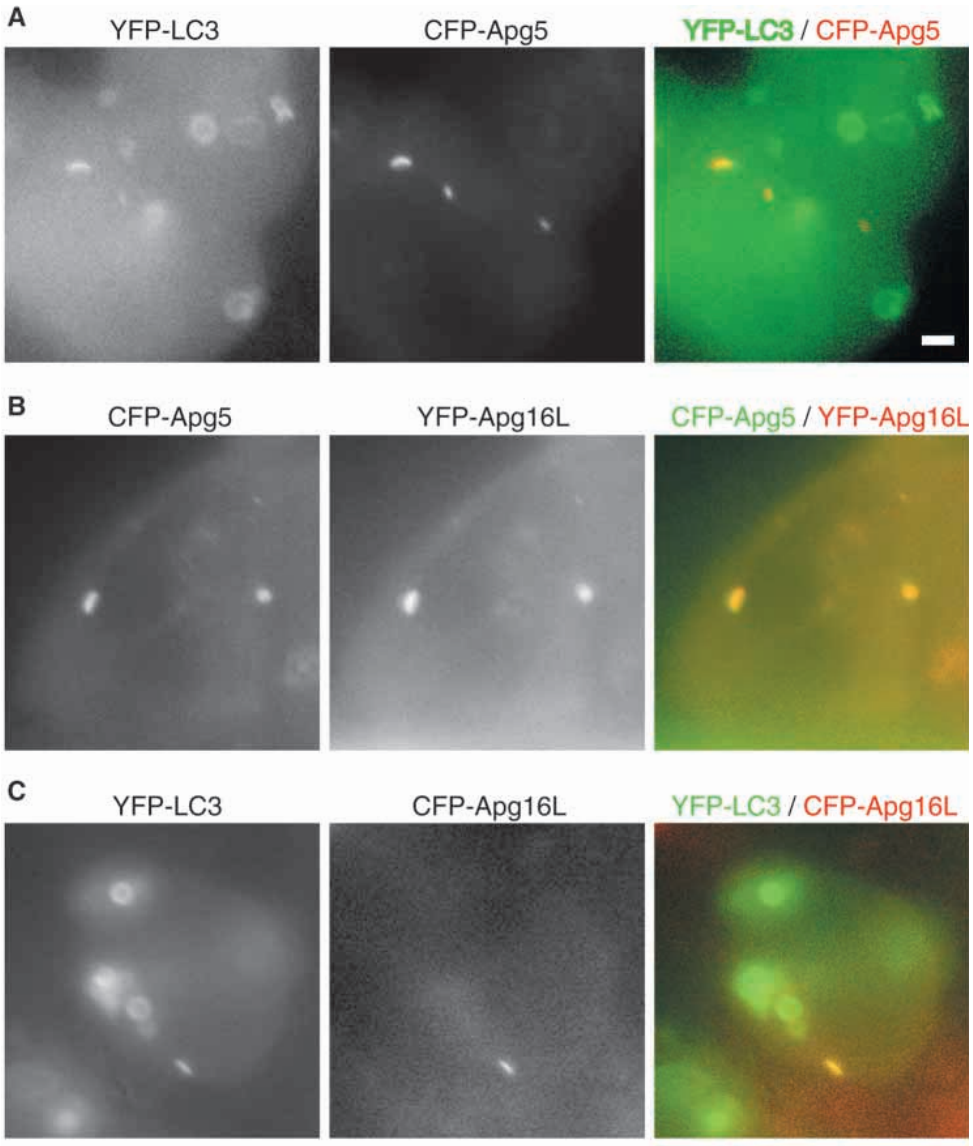

Fig. 6. Apg16L co-localizes completely with Apg5 and in part with LC3. ES cells stably co-expressing YFP-LC3 and CFP-Apg5 (A; clone F1-3), CFP-Apg5 and YFP-Apg16L (B; clone Y63D-3), and YFP-LC3 and CFP-Apg16L (C; clone B3-1-5) were cultured in Hanks' solution for 2 hours. Living cells were directly observed with a DeltaVision microscope system. ES cells grow as colonies; 4-7 cells are shown in each panel. Bars, 2 μm.

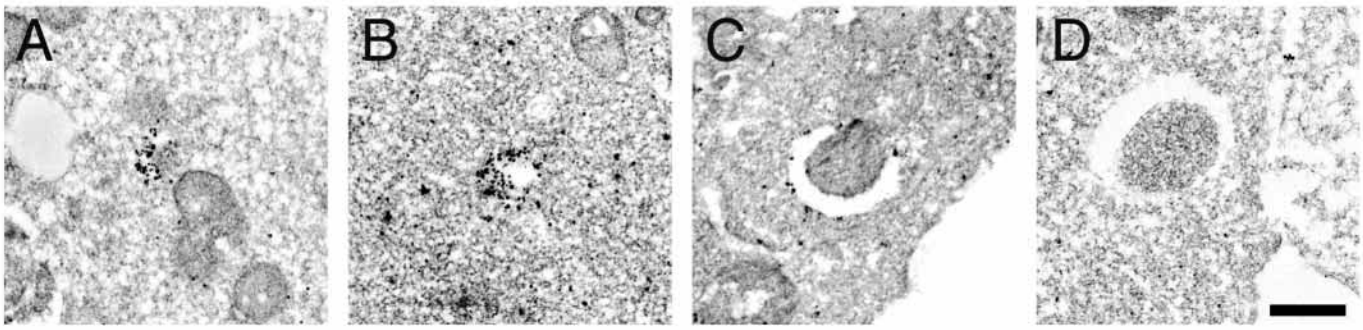

Fig. 7. GFP-Apg16L is present on isolation membranes. ES cells stably expressing GFP-Apg16L were cultured in Hanks' solution for 2 hours and then fixed with 4% paraformaldehyde. The localization of GFP-Apg16L was examined by silver-enhanced immunogold electron microscopy using an anti-GFP antibody. (A,B) Isolation membranes at very early stages. (C) Cup-shaped isolation membrane. (D) Autophagosome. Bar, 1 μm.

asymmetric, as observed for Apg5 (Mizushima et al., 2001). Apg16L was primarily found on the outer membrane of the cup-shaped isolation membrane, with only a little on the inner membrane (Fig. 7C). Apg16L was absent from the completed autophagosomal membrane (Fig. 7D) and autolysosomes (data not shown). These results suggest that Apg16L, in conjunction with the Apg12-Apg5 conjugate, localizes to the autophagic isolation membrane at the beginning of elongation and dissociates from the membrane at the completion of autophagosome formation.

Membrane targeting of Apg16L requires Apg5 but not Apg12 conjugation

To examine the membrane targeting of Apg16L further, we examined endogenous Apg16L by indirect immunofluorescence microscopy. GFP-Apg5-expressing ES cells were stained with an antibody against Apg16L. Apg16L staining co-localized with the GFP-Apg5 dots. There were no nonspecific dots (Fig. 8A), validating the specificity of the antibody. Using this antibody, we determined the role of Apg5 in the membrane association of Apg16L. Wild-type ES cells exhibited the formation of numerous Apg16L dots after 1 hour of amino acid starvation (Fig. 8C). By contrast, no punctate spots were observed in *APG5*$^{-/-}$ ES cells (Fig. 8D), suggesting that Apg5 is required for the membrane targeting of Apg16L.

We reported previously that Apg12 conjugation is not required for the membrane targeting of Apg5 using *APG5*$^{-/-}$ ES cells stably expressing a GFP-labeled, conjugation-defective Apg5^{K130R}, in which the Apg12 acceptor lysine residue was replaced (clone GKR-1) (Mizushima et al., 2001). Using these cells, we also examined the role of the Apg12-conjugation of Apg5 in the membrane association of Apg16L. In GKR-1 cells, the accumulating small GFP-positive structures (autophagosome precursors) were well stained with anti-Apg16L antibodies (Fig. 8B), suggesting that membrane targeting of Apg16L requires Apg5, but not a covalent attachment with Apg12.

Discussion

In this study, we identified a novel Apg5-interacting protein in mammalian cells. We named it Apg16L simply because it shows partial homology with yeast Apg16. Although Apg16L is much larger than yeast Apg16, we later concluded that it is indeed a functional counterpart of yeast Apg16, based on the following observations: (i) Apg16L forms a homo-oligomer, probably through the coiled-coil region; (ii) the N-terminal

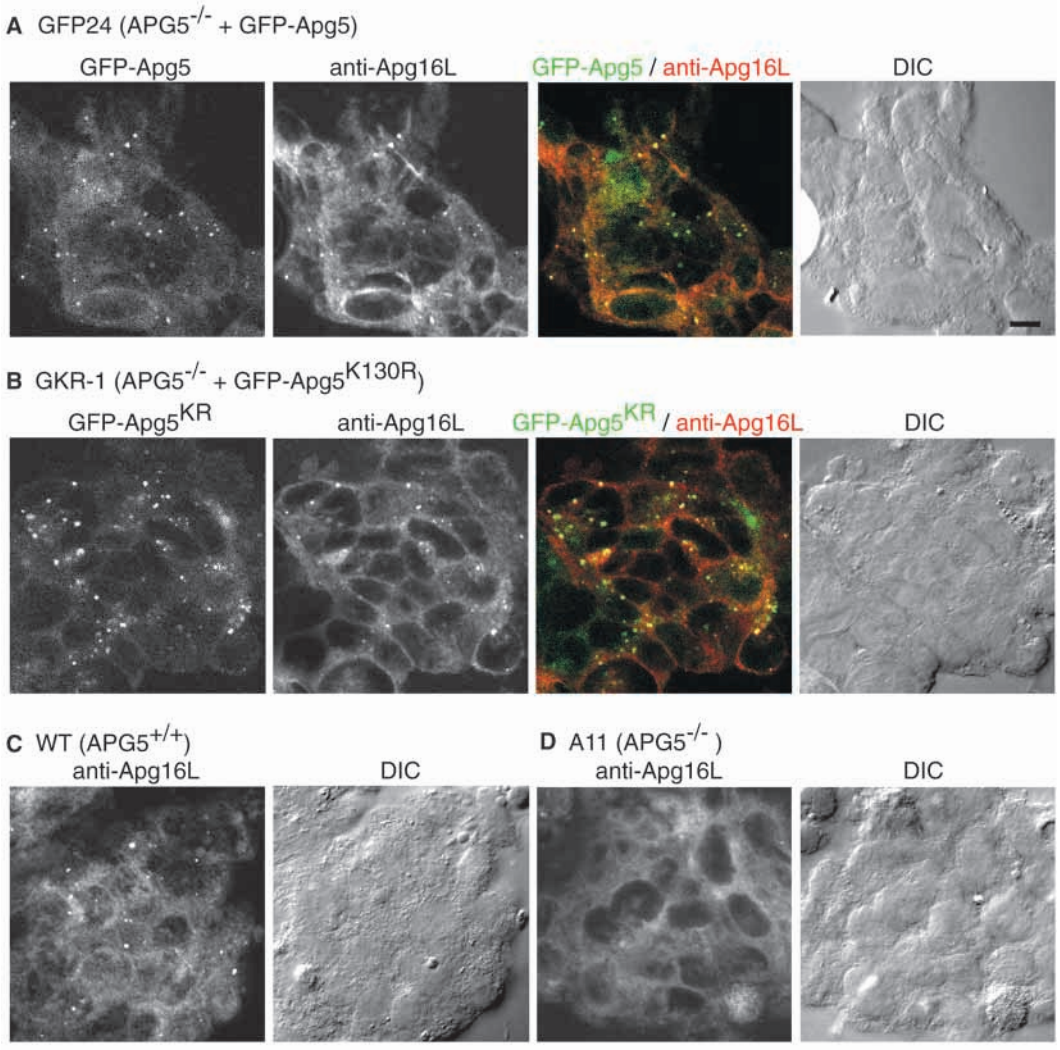

Fig. 8. Membrane association of Apg16L depends on Apg5 but not on Apg5 conjugation with Apg12. *APG5*$^{-/-}$ ES cells stably expressing GFP-Apg5 (GFP24) (A) or GFP-Apg5^{K130R} (GKR-1) (B), wild-type ES cells (C) and *APG5*$^{-/-}$ ES cells (D) were cultured in Hanks' solution for 2 hours. The cells were fixed, permeabilized and subjected to immunofluorescence confocal microscopy using an antiserum against Apg16L (p63C-2) and Cy5-conjugated goat anti-rabbit IgG secondary antibody. GFP-Apg5(KR) labeling, Apg16L staining, merged, and differential interference contrast (DIC) images are shown. Bars, 10 μm.

domain of Apg16L upstream of the coiled-coil region interacts with Apg5; (iii) Apg16L is a stoichiometric subunit of a large protein complex containing Apg12-Apg5. All these features are shared with yeast Apg16. Mammalian Apg16L, however, cannot replace Apg16 in yeast cells (data not shown). This might be partly because mouse Apg16L cannot interact with yeast Apg5 in yeast two-hybrid analysis (data not shown).

Multiple homologs of Apg16L in higher eukaryotes possess WD repeats in the C-terminal region, which is absent from yeast Apg16. This motif, first identified in the β subunits of trimeric G proteins, forms a β-propeller structure, which creates a stable platform for simultaneous interactions with multiple proteins (Smith et al., 1999). This symmetrical structure usually consists of at least four, and typically seven, repeats. Because the WD domain of Apg16L is not involved in either the interaction with Apg5 or homo-oligomerization, it is likely that unknown protein(s) interact with the WD domain. Purification of the ~800 kDa complex, however, demonstrated that Apg12, Apg5 and Apg16L are the main components (Fig. 1). Therefore, the putative WD-domain-binding protein might interact with only a small population of the total Apg12-Apg5·Apg16L complex, or might interact with the complex transiently. One attractive idea is that this protein might be a receptor for the Apg12-Apg5·Apg16L complex on the isolation membrane. Alternatively, the Apg12-Apg5·Apg16L complex might interact with this protein in the cytosol. The p144 protein (Fig. 1) remains a good candidate; we are now attempting both its purification and identification. Binding of p144 might then promote membrane association of the complex.

S. cerevisiae Apg16 lacks the C-terminal WD-repeat domain. Paz3, an Apg16 homolog in *Pichia pastoris*, also lacks this region (Mukaiyama et al., 2002) (Y. Sakai, personal communication). Higher-eukaryotic Apg16L might contain a WD domain because the putative binding partners of this domain might mediate additional autophagic machinery specific to higher eukaryotes. The several differences in autophagosome formation between yeast and mammalian cells might be controlled by this WD-repeat-containing region. Yeast autophagosomes are generated from a single preautophagosomal structure in the perivacuolar region, whereas several autophagosomes can be generated at the same time from multiple sites in mammalian cells. The size variation of autophagosomes is also much larger in mammalian cells than in yeast cells. Therefore, higher eukaryotes might have developed extra machinery creating these inherent differences from yeast in autophagosome formation. In addition, an unidentified WD-repeat protein corresponding to the C-terminal half of Apg16L might function together with Apg16 in yeast. Genome sequencing revealed that yeast has at least 60 WD-repeat proteins, many of unknown function. It is also possible that a short segment at the extreme C-terminal region (downstream of the coiled-coil region) of yeast Apg16 could exert a function corresponding to that of the Apg16L WD domain.

The mammalian Apg12-Apg5·Apg16L complex (~800 kDa) is much larger than the yeast complex (~350 kDa). Because it is unlikely that other molecules are involved in the formation of this mammalian complex (Fig. 1), we speculate that the ~800 kDa complex contains eight sets of Apg12-Apg5·Apg16L, whereas the ~400 kDa minor complex (Fig. 5B) contains four sets. If so, the minor ~400 kDa complex might contain equivalent components to the yeast complex; most of these complexes would then doubly associate in mammalian cells.

Apg16L is expressed in different isoform patterns in mouse depending on the tissue. We identified three isoforms produced by alternative splicing. We could not discern any differences among these isoforms in complex formation; each can be incorporated into the ~800 kDa complex. The possibility remains, however, that the Apg16L isoforms differ in additional functions.

The intracellular localization of Apg16L is exactly the same as that of Apg5, indicating that the Apg12-Apg5·Apg16L complex localizes to the autophagosome precursors, remaining there until autophagosome formation is completed. In yeast, the membrane targeting of Apg5 requires Apg16 (Suzuki et al., 2001). We thought that Apg16 might function as a membrane anchor for Apg5. Apg16L, however, is unable to associate with membranes in Apg5-deficient ES cells. Therefore, Apg16L alone is not sufficient for membrane association. Apg12 conjugation of Apg5, however, is dispensable for the membrane targeting of Apg5 and Apg16L. Thus, the interaction between Apg5 and Apg16L is necessary and sufficient for the binding of Apg16L to the isolation membranes. Apg12 conjugation, although it is dispensable for membrane association, is required for the involvement of the Apg5·Apg16L complex in isolation membranes elongation (Mizushima et al., 2001).

Identification of Apg16L not only acquires a missing Apg homolog but also gives additional clues pertinent to understanding the molecular mechanism of autophagy. The future identification of putative WD-domain-binding proteins will provide valuable information about the function of the Apg12-Apg5·Apg16L complex in autophagosome formation and possible higher-eukaryote-specific activities of these proteins.

We thank Philip James (University of Wisconsin) for providing the yeast strains and vectors necessary for the yeast two-hybrid analysis, Andras Nagy (Samuel Lunenfeld Research Institute) for kindly providing the R1 ES cells, Allan Bradley (Baylor College of Medicine) for donation of the pPGKpurobpA plasmid, Sumio Sugano (The Institute of Medical Science, The University of Tokyo) for his kind gift of the pCE-FL vector and Yasuyoshi Sakai (Kyoto University) for providing the amino acid sequence of *P. pastoris* Paz3 before publication. This work was supported in part by Grants-in-aid for Scientific Research from the Ministry of Education, Culture, Sports, Science and Technology of Japan.

References

Blommaart, E. F. C., Luiken, J. J. F. P. and Meijer, A. J. (1997). Autophagic proteolysis: control and specificity. *Histochem. J.* **29**, 365-385.

Dunn, W. A. J. (1994). Autophagy and related mechanisms of lysosome-mediated protein degradation. *Trends Cell Biol.* **4**, 139-143.

Ichimura, Y., Kirisako, T., Takao, T., Satomi, Y., Shimonishi, Y., Ishihara, N., Mizushima, N., Tanida, I., Kominami, E., Ohsumi, M. et al. (2000). A ubiquitin-like system mediates protein lipidation. *Nature* **408**, 488-492.

James, P., Halladay, J. and Craig, E. A. (1996). Genomic libraries and a host strain designed for highly efficient two-hybrid selection in yeast. *Genetics* **144**, 1425-1436.

Kabeya, Y., Mizushima, N., Ueno, T., Yamamoto, A., Kirisako, T., Noda, T., Kominami, E., Ohsumi, Y. and Yoshimori, T. (2000). LC3, a mammalian homologue of yeast Apg8p, is localized in autophagosome membranes after processing. *EMBO J.* **19**, 5720-5728.

Kim, J., Dalton, V. M., Eggerton, K. P., Scott, S. V. and Klionsky, D. J. (1999). Apg7p/Cvt2p is required for the Cvt, macroautophagy, and peroxisome degradation pathway. *Mol. Biol. Cell* **10**, 1337-1351.

Kirisako, T., Ichimura, Y., Okada, H., Kabeya, Y., Mizushima, N., Yoshimori, T., Ohsumi, M., Takao, T., Noda, T. and Ohsumi, Y. (2000). The reversible modification regulates the membrane-binding state of Apg8/Aut7 essential for autophagy and the cytoplasm to vacuole targeting pathway. *J. Cell Biol.* **151**, 263-275.

Klionsky, D. J. and Emr, S. D. (2000). Autophagy as a regulated pathway of cellular degradation. *Science* **290**, 1717-1721.

Kuma, A., Mizushima, N., Ishihara, N. and Ohsumi, Y. (2002). Formation of the ~350 kD Apg12-Apg5·Apg16 multimeric complex, mediated by Apg16 oligomerization, is essential for autophagy in yeast. *J. Biol. Chem.* **277**, 18619-18625.

Mizushima, N., Noda, T., Yoshimori, T., Tanaka, Y., Ishii, T., George, M. D., Klionsky, D. J., Ohsumi, M. and Ohsumi, Y. (1998a). A protein conjugation system essential for autophagy. *Nature* **395**, 395-398.

Mizushima, N., Sugita, H., Yoshimori, T. and Ohsumi, Y. (1998b). A new protein conjugation system in human. The counterpart of the yeast Apg12p conjugation system essential for autophagy. *J. Biol. Chem.* **273**, 33889-33892.

Mizushima, N., Noda, T. and Ohsumi, Y. (1999). Apg16p is required for the function of the Apg12p-Apg5p conjugate in the yeast autophagy pathway. *EMBO J.* **18**, 3888-3896.

Mizushima, N., Yamamoto, A., Hatano, M., Kobayashi, Y., Kabeya, Y., Suzuki, K., Tokuhisa, T., Ohsumi, Y. and Yoshimori, T. (2001). Dissection of autophagosome formation using Apg5-deficient mouse embryonic stem cells. *J. Cell Biol.* **152**, 657-667.

Mizushima, N., Ohsumi, Y. and Yoshimori, T. (2002a). Autophagosome formation in mammalian cells. *Cell Struct. Funct.* **27**, 421-429.

Mizushima, N., Yoshimori, T. and Ohsumi, Y. (2002b). Mouse Apg10 as an Apg12 conjugating enzyme: analysis by the conjugation-mediated yeast two-hybrid method. *FEBS Lett.* **532**, 450-454.

Mukaiyama, H., Oku, M., Baba, M., Samizo, T., Hammond, A. T., Glick, B. S., Kato, N. and Sakai, Y. (2002). Paz2 and 13 other *PAZ* gene products regulate vacuolar engulfment of peroxisomes during micropexophagy. *Genes Cell* **7**, 75-90.

Natsume, T., Yamauchi, Y., Nakayama, H., Shinkawa, T., Yanagida, M., Takahashi, N. and Isobe, T. (2002). A direct nanoflow liquid chromatography-tandem mass spectrometry system for interaction proteomics. *Anal. Chem.* **74**, 4725-4733.

Ohsumi, Y. (2001). Molecular dissection of autophagy: two ubiquitin-like systems. *Nat. Rev. Mol. Cell. Biol.* **2**, 211-216.

Seglen, P. O. and Bohley, P. (1992). Autophagy and other vacuolar protein degradation mechanisms. *Experientia* **48**, 158-172.

Shintani, T., Mizushima, N., Ogawa, Y., Matsuura, A., Noda, T. and Ohsumi, Y. (1999). Apg10p, a novel protein-conjugating enzyme essential for autophagy in yeast. *EMBO J.* **18**, 5234-5241.

Smith, T. F., Gaitatzes, C. G., Saxene, K. and Neer, E. J. (1999). The WD-repeat: a common architecture for diverse functions. *Trends Biol. Sci.* **24**, 181-185.

Suzuki, K., Kirisako, T., Kamada, Y., Mizushima, N., Noda, T. and Ohsumi, Y. (2001). The pre-autophagosomal structure organized by concerted functions of *APG* genes is essential for autophagosome formation. *EMBO J.* **20**, 5971-5981.

Tanida, I., Mizushima, N., Kiyooka, M., Ohsumi, M., Ueno, T., Ohsumi, Y. and Kominami, E. (1999). Apg7p/Cvt2p: a novel protein-activating enzyme essential for autophagy. *Mol. Biol. Cell* **10**, 1367-1379.

Tanida, I., Tanida-Miyake, E., Ueno, T. and Kominami, E. (2001). The human homolog of *Saccharomyces cerevisiae* Apg7p is a protein-activating enzyme for multiple substrates including human Apg12p, GATE-16, GABARAP, and MAP-LC3. *J. Biol. Chem.* **276**, 1701-1706.

Tanida, I., Tanida-Miyake, E., Komatsu, M., Ueno, T. and Kominami, E. (2002). Human Apg3p/Aut1p homologue is an authentic E2 enzyme for multiple substrates, GATE-16, GABARAP, and MAP-LC3, and facilitates the conjugation of hApg12p to hApg5p. *J. Biol. Chem.* **277**, 13739-13744.

Thumm, M., Egner, R., Koch, B., Schlumpberger, M., Straub, M., Veenhuis, M. and Wolf, D. H. (1994). Isolation of autophagocytosis mutants of *Saccharomyces cerevisiae*. *FEBS Lett.* **349**, 275-280.

Tsukada, M. and Ohsumi, Y. (1993). Isolation and characterization of autophagy-defective mutants of *Saccharomyces cerevisiae*. *FEBS Lett.* **333**, 169-174.

Wolf, E., Kim, P. S. and Berger, B. (1997). MultiCoil: a program for predicting two- and three-stranded coiled coils. *Protein Sci.* **6**, 1179-1189.

Yoshimori, T., Yamagata, F., Yamamoto, A., Mizushima, N., Kabeya, Y., Nara, A., Miwako, I., Ohashi, M., Ohsumi, M. and Ohsumi, Y. (2000). The mouse SKD1, a homologue of yeast Vps4p, is required for normal endosomal trafficking and morphology in mammalian cells. *Mol. Biol. Cell* **11**, 747-763.

Yuan, W., Stromhaug, P. E. and Dunn, W. A., Jr (1999). Glucose-induced microautophagy of peroxysomes in *Pichia pastoris* requires a unique E1-like protein. *Mol. Biol. Cell* **10**, 1353-1366.